REPORT DOCUMENTATION PAGE

Form Approved
OMB No. 0704-0188

1. REPORT DATE *(DD-MM-YYYY)*	2. REPORT TYPE	3. DATES COVERED *(From - To)*
	Technical Paper	

4. TITLE AND SUBTITLE	5a. CONTRACT NUMBER F04611-96-C-0001
	5b. GRANT NUMBER
	5c. PROGRAM ELEMENT NUMBER
6. AUTHOR(S)	5d. PROJECT NUMBER
	5e. TASK NUMBER
	5f. WORK UNIT NUMBER
7. PERFORMING ORGANIZATION NAME(S) AND ADDRESS(ES) Sverdrup	8. PERFORMING ORGANIZATION REPORT
9. SPONSORING / MONITORING AGENCY NAME(S) AND ADDRESS(ES) Air Force Research Laboratory (AFMC) AFRL/PRS 5 Pollux Drive Edwards AFB CA 93524-7048	10. SPONSOR/MONITOR'S ACRONYM(S)
	11. SPONSOR/MONITOR'S NUMBER(S)

12. DISTRIBUTION / AVAILABILITY STATEMENT

Approved for public release; distribution unlimited.

13. SUPPLEMENTARY NOTES

14. ABSTRACT

15. SUBJECT TERMS

16. SECURITY CLASSIFICATION OF:			17. LIMITATION OF ABSTRACT	18. NUMBER OF PAGES	19a. NAME OF RESPONSIBLE PERSON
					Leilani Richardson
a. REPORT	b. ABSTRACT	c. THIS PAGE	A		19b. TELEPHONE NUMBER *(include area code)*
Unclassified	Unclassified	Unclassified			(661) 275-5015

NUMERICAL INVESTIGATION OF TWIN-NOZZLE ROCKET PLUME PHENOMENOLOGY

Houshang B. Ebrahimi
Sverdrup Technology, Inc./AEDC
Arnold Engineering Development Center
Arnold Air Force Base, TN 37389-6001

Jay Levine
Air Force Research Laboratory
Edwards AFB, CA 93524

And

Alan Kawasaki
Sparta, Inc.
Edwards AFB, CA 93524

ABSTRACT

The Generalized Implicit Flow Solver (GIFS) computer program has been modified and applied for the analysis of three-dimensional reacting two-phase flow simulation problems. The intent of the original GIFS development effort was to provide the Joint Army, Navy, NASA, Air Force (JANNAF) community with a standard computational methodology to simulate the complete flowfield of propulsion systems including multiple nozzle/plume flow field phenomena and other three-dimensional effects. The Van Leer Flux Splitting option has been successfully implemented into the existing GIFS model and provides a more robust solution scheme, making application of the model more reasonable for engineering applications.

This paper reports the significant results of several twin-nozzle/plume simulations using the GIFS code. Eight simulations of Titan II plume flow fields have been completed to assess the effects of three-dimensionality, turbulent viscosity, afterburning, near-field shock structure, finite-rate kinetic chemistry, internozzle geometric spacing, nozzle exit plane profile, and missile body on the subsequent plume exhaust flow field. The results of these calculations indicate that the viscous stress model, kinetic chemistry especially at lower altitudes, and nozzle exit profile are important parameters that should be considered in the analyses and the interpretation of the calculations. Three-dimensionality is also an important influence, which can substantially influence the interpretation of the results. If three-dimensional effects are oversimplified in the model, analyses of the spatial results can be misinterpreted and misapplied. In addition, the missile body effect and internozzle geometric spacing influence the expansion shock reflection location which can significantly affect the plume/plume impingement shock location, inviscid shock structure, and shear layer growth.

INTRODUCTION

In order to support propulsion testing and analysis requirements of the aerospace and exhaust plume communities, a need exists for a fluid dynamics model that solves the fully coupled, two-phase Navier-Stokes equations in multiple dimensions. Evaluation of solid-propellant rocket motor performance and rocket plume radiative transfer analyses require a computer model that simulates complex three-dimensional, chemically reacting two-phase flow effects.[1] In the past few years, significant progress has been made in the areas of numerical rocket flow simulations and computational resources to the point that Navier-Stokes solutions are viable analysis tools. Although this type of full Navier-Stokes method provides an accurate qualitative description of the basic features of the propulsion-generated flow fields, quantitative simulations for predicting fundamental parameters such as base pressure and heat transfer, gas static pressure, gas and particulate temperatures, and chemical composition in the flow field domain have not been validated.

The flow fields generated by rocket propulsion systems are complex, with regions of strong inviscid/viscous interactions, free-stream shear layers, nozzle wall and missile body boundary layers, external and internal shocks, separation regions, and plume/plume impingement and associated flow interactions for multiple nozzle designs, all with chemically reacting kinetics.[2] Coupling all of these phenomena simultaneously in a numerical simulation tool challenges the state-of-the-art (SOA) for CFD models. To account for the significant phenomena affecting plume flow properties and the resulting radiative transfer implications, computationally efficient multi-dimensional computer models are required.

Recently there has been increased emphasis on the application of existing CFD models, both in the commercial arena and government-developed computer programs, to simulate complex multidimensional plume phenomena. A large majority of the solutions obtained to date are based on the perfect gas (constant gamma) approximation, as fully reacting flows are considerably more complex and difficult to solve. Including the effects of chemistry in the solution produces a stiff set of equations that are numerically difficult to solve using conventional algorithms. In addition, the grid resolution requirements become more severe, and time step issues arise when reacting chemistry is included in the Navier-Stokes model.

Conventional rocket exhaust flow computer models[3,4] employ Euler solutions for the inviscid plume core flow region. Overlaid onto the inviscid solution is an uncoupled, parabolic mixing methodology for the turbulent, chemically reacting, free-stream air entrainment in the shear layer region. These methods are generally not adequate for situations when the flow is not fully dominated by either inviscid core gasdynamics or the plume afterburning phenomena. Three-dimensional features produced by multiple nozzle propulsion systems and vehicle body/base interactions cannot be sufficiently treated through the use of these models. Inaccurate accounting of the 3D upstream influences on the plume shear layer development and the resulting plume structure is one of the primary issues preventing approximate models from accurately simulating the overall flow field phenomena[5].

The GIFS numerical algorithm provides a solution of the two- and three-dimensional Reynolds-averaged Navier-Stokes (NS) equations using the MacCormack implicit finite-volume algorithm with Gauss-Seidel line relaxation.[6] Several 2-D and 3-D plume flow-field calculations have been completed for the plume near-field region using the original version of the GIFS model.[6] The GIFS model includes a frozen and a generalized finite-rate kinetic chemistry model, a Lagrangian particle model for treating solid and liquid particulates, and a two-equation Kε turbulence model, as well as a laminar flows. These complex phenomena are required to accurately simulate the physics expected to contribute to the flow-field spatial distribution of gas dynamic, thermodynamic, and chemical properties. The Van Leer Flux Splitting option[7] has been successfully implemented into the original GIFS model and provides a more robust solution scheme for simulating propulsion flow-field phenomena.[8] Convergence characteristics, using the Van Leer scheme, are vastly improved particularly in regions of high property gradients, where the solution stabilizes more rapidly, and thereby allows the use of larger CFL values.

The enhanced version of the GIFS model was applied in this study. A previous investigation [8] focused on the validation of the enhanced version of the GIFS model using an extensive database of laboratory measurements. The validation focused on the combustion, turbulence and three-dimensional aspects of the model. Comparisons of the GIFS calculation results with the measurements were encouraging.

The near-field plume flow field emanating from a multi-nozzle vehicle flying at high altitude is largely dominated by the processes taking place in the plumes' interaction region. Prior to the release of the GIFS model, simulations of multiple nozzle/plume flow fields were commonly treated by assuming a single equivalent nozzle configuration having equal mass, energy, and momentum of the multiple nozzle geometry. Further, as a simplifying assumption, uniform (one-dimensional) nozzle exit flow properties were used as the starting conditions for the plume calculation. The simplified model assumes that the details of the 3-D flow structure in the near-field region and the uniform start condition are unimportant and that the flow processes affecting the plume shear layer initialization (such as base separation and recirculation) will be dominated by the overall ambient flow entrainment effects. For analyses requiring spatial detail and accuracy, the level of agreement between computations based on the simplified single equivalent nozzle methodology and simulations from multiple nozzle propulsion systems has not been acceptable. The source of the disagreement is due, at least in part, to an incorrect physical model of the phenomena dominating the observations, e.g., inadequate turbulence, incomplete chemical mechanisms, missing or inaccurate reaction rates, simplified initial start conditions and three-dimensional geometry effects. The actual physical geometries are often oversimplified, and relevant details of the engine design and the resulting impact on the initial conditions and the down-stream exhaust flow are frequently ignored.

The motivation for this study is to demonstrate the significance of three-dimensional effects as applied to multiple nozzle missile plumes in order to determine

how these phenomena may be simplified and incorporated into engineering analysis models. The knowledge gained can be applied to promote improvements to engineering approaches and to explore methods to reduce the overall CPU resource requirements for three-dimensional computer simulations. While it is recognized that grid issues affect the solution integrity, grid refinement was not a part of this study.

COMPUTATIONS

The computational effort consisted of seven, three-dimensional twin-nozzle simulations and one 2-D axisymmetric calculation for the Titan II vehicle at flight conditions. In the first six cases, only the plume flow field was computed, i.e., missile base effects were not considered. Also, in the first five cases, boundary-layer effects from inside the rocket nozzle were not considered. The starting boundary conditions at the nozzle exit plane were assumed to be uniform for these cases. In the sixth case, the plume flowfield was computed utilizing a two-dimensional, viscous radial profile starting conditions at the nozzle exit plane. The GIFS model was initiated at the nozzle exit plane using results obtained from the Two Dimensional Kinetic computer program[9] .The GIFS model was then applied to simulate the external plume flowfield. For all cases, the plume flow field was simulated at an altitude of 47.6 km and the vehicle Mach number was 5.7. The nozzle operated in a significantly underexpanded mode ($Pe>>P\infty$). In the first six cases, the resulting nozzle exit-to-free-stream velocity ratio was approximately 5, and the chamber pressure to free-stream pressure ratio was approximately 50,000:1. In the last 3-D case, a complete solution, including the external flow over the missile body, the base region, and the gas generator flow was included in this simulation. To provide a contrasting solution to the 3-D flowfield simulations, an axisymmetric approximation for the dual nozzle plumes was computed. In this case, the mass flow from the dual engine was matched by scaling up the engine dimensions by $\sqrt{2}$. The parametric flow field conditions and assumptions for all eight cases are summarized in Table 1.

The Titan II Space-Launched Vehicle (SLV) propulsion system is propelled by two engines located on either side of a plane of symmetry passing through the vehicle centerline. Figure 1 is a schematic of the vehicle. The sea-level rated thrust derived from each engine is approximately 214,000 lbf. Roll, pitch, and yaw control are provided by gimballing of the engine ±5 degrees from the engine neutral position (2 degree cant angle away from the vehicle centerline for both nozzles). The 2-deg cant angle was included in the three-dimensional simulations.[10] Both nozzles are identical in geometry and operating conditions.

The thrust chamber assemblies and nozzle skirt are regeneratively cooled. In addition, injector spray patterns intentionally direct a fuel rich layer adjacent to the chamber walls to reduce the wall heat loads. The engine fuel is AEROZINE-50, a 50/50 blend of hydrazine (N_2H_4) and unsymmetrical dimethylhydrazine ($C_2H_8N_2$), and the oxidizer is N_2O_4. Power to drive the turbopumps is derived from two gas generators, which represent approximately 1.5 percent of the overall propellant expended by both

engines. These gas generators are intentionally operated at fuel-rich conditions to minimize heat leads on the turbine blades.

To limit the number of grid points and CPU run time, quarter symmetry assumptions were made for the computational domain plane. Zero angle of attack and dual plume exhaust were two additional constraints imposed for these simulations. A total of 600,000 grid points were utilized in the computational domain for the first six cases, 4 million grid points for the last 3-D case, and 200,000 grid points for the axisymmetric case. It should be noted that for the three characteristic cases (ie., 3-D flying plume, 3-D plume with body, and the axisymmetric plume with body) the grid resolution was not consistently set. The 600,000 node grid was quite coarse for the 3-D flying plume cases, but for the purposes of making qualitative comparisons between similar cases (cases 1 thru 6), the basic features from these solutions appeared to be adequately resolved. In the last 2 cases, grid resolution was sufficiently refined. The exhaust plume portion of the computational domain is shown in Fig. 2a with the orientation indicated by the axes. A schematic of the 3-D plume configuration is shown in Fig. 2b.

External airflow conditions, engine nozzle exit conditions, throat conditions, and gas generator conditions for the Titan test cases are presented in Table 2. The finite-rate chemical kinetic simulations used a chemical reaction model consisting of 11 species and 210 reactions for carbon, hydrogen, oxygen, and nitrogen-based propellant systems[9]. The rate-controlled reactions included the recombination and dissociation of 9 species: CO, CO_2, N_2, H_2, H, H_2O, OH, O_2, and O. Two additional compounds, methane (CH_4) and ammonia (NH_3), were included as part of the overall mixture, for completeness. However, neither methane nor ammonia were allowed to react within the flow exhaust. Since these species were in small concentrations, it was assumed that the decomposition of these species would not significantly contribute to the heat release nor alter the mixture sufficiently to impact the overall simulation.

The K-ε turbulence model[11] was applied for viscous stress approximation. The computation was performed on a single processor SGI Power Challenge R8000. For the first six cases, the calculations executed for approximately 11,000 iterations. Case 7, the three-dimensional calculation including the missile body/base and gas generator, was the most stressing case. This solution required approximately three months of CPU time to converge. In contrast, the axisymmetric case required 4 days to converge.

Seven three-dimensional numerical calculations of the twin-nozzle configuration were obtained at Mach 5.7 for different combinations of flow assumptions and approximations in an attempt to isolate individual influences and effects. Cases 1 and 2 compare laminar flow and turbulent viscous stress models, respectively, and were computed assuming a perfect gas equation of state. Case 3 is a turbulent, constant-gamma approximation with an internozzle geometric spacing that differed from Cases 1 and 2. Cases 4 and 5 contrast frozen- and finite-rate chemistry, respectively. Cases 1-5 all assume uniform nozzle exit properties as the GIFS start line conditions. Case 6 is a

chemically reacting plume exhaust using two-dimensional, radially-varying viscous profiles for the initial conditions at the nozzle exit plane location (calculated via TDK) to define the starting boundary condition for the GIFS plume calculation. The final 3D case (Case 7) simulated the flowfield over the missile body, the base region, and the exhaust plume domains including the fuel-rich gas generator flow and chemical kinetics. Case 8 assumed a single equivalent nozzle approximation for the twin nozzle configuration. Cases 7 and 8, both, were initialized at the nozzle throat using a uniform inflow condition. The resulting 2-D profile at the nozzle exit were comparable to the 2-D profiles used by Case 6.

The following sections will discuss the individual influences of the various assumptions for phenomena simulated in the GIFS model.

THREE-DIMENSIONAL EFFECT

In an earlier study by one of the authors[2] and others[12], it was shown that three-dimensional effects are significant and should not be ignored or oversimplified in modeling efforts. Figure 3 shows Mach contours for the three-dimensional solution. The plume expansion shock, barrel shock, and shock reflection are clearly visible at 116 meters downstream of the nozzle exit plane location. The static temperature is increased downstream of the reflection point approaching a value slightly less than half the value of the total temperature of the flow. A comparison of the two-dimensional axisymmetric solution with the three-dimensional twin-nozzle solution was accomplished to determine the impact of the single equivalent nozzle assumption. Figure 4 provides a comparison of the axisymmetric and the 3-D solutions. There are significant differences between the two solutions, including the plume size, asymmetric flow distributions, and the location of the shock reflection points. Though these differences may infer that the axisymmetric solutions are inaccurate, the 2-D assumptions do provide insight concerning overall gross qualitative assessments, such as similarties in the barrel shock features and the global farfield properties. For parametric studies, axisymmetric simulations are often dictated due to time and computer resource constraints, but for detailed studies requiring accurate spatial resolution of multi-nozzle flows or flows with angle of attack, three-dimensional calculations are required.

TURBULENCE EFFECT

In order to assess the influence of turbulence in the plume flow-field solution resulting from twin nozzles, two three-dimensional calculations were performed, one assuming turbulent flow and the other assuming laminar flow. As would be expected, comparisons of the flow-field results for the turbulent and laminar cases, shown in figure 5, indicate decreasing trends in plume impingement intensity and plume mixing rate for the laminar calculation.

The comparison of static pressure contours in the horizontal and cross-planes is shown in Fig. 5. The turbulent and the laminar solutions are displayed in the same plot and are separated by Z = 0 line. Static temperature centerline axial profiles contrasting

the turbulent and laminar solutions are shown in Fig. 6. These results indicate that the barrel shock reflection point is located approximately 8 meters farther downstream for the turbulent solution. Therefore, the spatial characteristics of the plume flow field and, hence, the location of the radiation centroid can be influenced by the viscous stress model. The influence of different turbulence models was not assessed. The Kε-two equation turbulence model[11] was applied exclusively in this study. In the present case at 47.6-km altitude, the effect of turbulence is not particularly strong. However, at lower altitudes and, hence, higher Reynolds numbers, turbulent effects will be more significant.

INTERNOZZLE GEOMETRIC SPACING EFFECT

The distance between the nozzles influences the location and strength of the plume/plume interactions. In order to explore this effect, perfect-gas, three-dimensional calculations were obtained at two different internozzle geometric spacings (narrow versus wide spacing). The variation in the distance between nozzle centerline locations for the two cases was approximately 15 percent with the first case assuming the widest separation distance. Figure 7 compares static temperature contours from the two solutions. These results indicate that internozzle spacing has a noticeable influence on the flow-field structure. As seen in Fig. 7, the initial plume expansion angle is larger for the wider spacing case, and the shock reflection location is farther downstream. A centerline axial profile of static temperature is displayed in Fig. 8, contrasting the two nozzle spacing solutions. The difference in the location of the shock reflection point is evident. Figure 8 also confirms that the increased static temperature of the wide spacing case extends throughout the calculation domain. It is concluded that the internozzle spacing affects the plume impingement shock location, the inviscid shock structure, and the shear layer development. Thus, relatively small differences in internozzle nozzle spacing can impact the flow field and it is likely to influence the plume radiative emissions.

REACTING FLOW EFFECT

A frozen-chemistry solution was contrasted with a finite-rate reacting solution to assess the significance of chemistry in complex plume flow fields. A comparison of the two calculations indicates that kinetic chemistry can affect the overall plume structure. Figure 9 is a centerline axial profile of static temperature extending from the nozzle exit plane to 150 meters downstream for the kinetic and the frozen chemistry assumption. This comparison indicates that the chemistry model has an effect on the location of the barrel shock reflection point. The barrel shock reflection from the plume centerline occurs farther upstream for the reacting flow solution compared with the frozen case. However, overall, the comparison between the reacting and the frozen cases indicates that chemistry effects are not as significant at this high altitude condition. At high altitudes, the oxygen content of the ambient air is reduced and the ambient temperature and pressure are low. These conditions are not conducive to shear layer combustion. It is expected that the chemistry effect will be more significant at lower altitudes, where plume/atmospheric afterburning will dominate the flow field.

NOZZLE EXIT BOUNDARY CONDITION PROFILE EFFECT

In a previous study by one of the authors[5] to assess phenomena affecting scramjet nozzle performance, it was determined that performance is sensitive to variations in the radial profiles assumed for the start line conditions. Thus, the influence of nozzle exit plane profile variations, assumed as starting conditions for the GIFS plume simulation, on the plume flow field was investigated. In one case, radially varying nozzle exit plane profiles were determined via the TDK code. In the second case, uniform (one-dimensional) nozzle exit plane profiles were assumed. The uniform conditions had the same mass, energy and momentum as the radially varying conditions. Plume expansions were then calculated for each case assuming fully turbulent, chemically reacting flow. Radial profiles of static temperature for both startline assumptions are shown at axial positions equal to 3, 10, and 20 meters downstream of the nozzle exit in Figure 10. A comparison of the spatial plume size indicates that the uniform start line results in a slightly larger radial plume-expansion due to the increased pressure difference between the nozzle exit and the free stream. As expected, differences between the two start-line approximations become less significant as the flow progresses axially downstream. Although these two solutions do not show a significant effect of exit profile shape on the plume temperature, it is expected that in other cases, especially those with strong afterburning, differences in the shear stress between the core flow and the ambient air stream could affect the mixing rates and consequently, the combustion chemistry in the shear layer. It should also be pointed out that the aforementioned solutions were obtained assuming constant oxidizer/fuel (O/F) ratio across the inflow plane. When real engine effects such as fuel-film cooling and injector imperfections are accounted for, O/F can vary widely across the nozzle exit plane. In order to properly account for the effect of mixture ratio variations on the plume flow field and the resulting base heat-transfer effects, radially varying oxidizer-to-fuel ratios should also be considered.

MISSILE BODY EFFECT

To assess the influence of the missile body and base region on the plume flow-field solution, a three-dimensional calculation was performed simulating the flow field over the missile body, the base region and the exhaust plume domain. This calculation also included the gas generator effluent. Figure 11a is static pressure in the missile base regions resulting from the nose-to-tail, three-dimensional solutions. Figures 11b and 11c are close-up views of Mach number vectors and static temperature contours, respectively, in the missile base flow region. The heating of the missile base surface and the effect of the gas generator effluent impinging on the nozzle surfaces are clearly evident. Further, the gas generator flow initially expands as it exits the nozzle, adjusting to the ambient pressure condition, but further downstream in the region between the two nozzles, the gas generator flow is compressed because of the area change created by the nozzle expansion skirt hardware. In Fig. 11b, showing the Mach vectors, the interaction of the gas

generator flow with base regions and the nozzles is apparent. This interaction creates recirculation of the hot gases into the missile base region, evident in Fig.11c. The blunt-body shock, plume expansion shock, and shock reflection and resulting recirculation region are evident. Figure 12 contrasts static temperature contours and centerline static temperature profiles with and without the missile body included in the solutions. These results indicate that the plume expansion angles are larger and the overall plume width is wider if the missile body and base region are included in the computational domain. The expansion shock reflection point on the plume centerline is located 12 m farther downstream in the solution including the body and base. It appears that the missile body effects are significant and influences the inviscid shock structure, including the location of the reflection of the plume expansion shock, and the plume shear layer development.

CONCLUSIONS

A modified three-dimensional GIFS model was applied extensively for this study which included seven different three-dimensional solutions and an axisymmetric approximation of the 3D geometry. The effects of nozzle exit plane nonuniformity, internozzle spacing, turbulence, finite-rate chemistry, and 3D geometry were evaluated for a twin nozzle/plume propulsion configuration at a high altitude flight condition. Analysis of the solutions isolating these various effects leads to the following conclusions:

1. Startline assumptions, two-dimensional radially varying versus one dimensional, uniform, had a significant effect on the immediate plume near field calculation. The differences between the solutions resulting from the varying start line assumption became less significant as the axial distance downstream of the nozzle exit plane increased. This significance of this sensitivity needs additional investigation to elucidate the effect of the starting conditions on the plume flow field, especially in the presence of strong afterburning and missile body/base flow field interactions.

2. Comparison of solutions contrasting laminar flow and turbulent flow indicates that plume flow field simulations are influenced by turbulence. Laminar flow approximations will degrade further at lower altitudes where turbulent mixing becomes more dominant.

3. The chemistry assumption (frozen versus reacting) did not significantly influence the overall plume structure in this high altitude simulation. Some minor differences were noted; however, at the high altitude flight condition simulated, chemistry effects are not dominate because the low pressure, cold temperature, and low atmospheric oxygen content of the ambient air are not conducive to shear layer combustion. At lower-altitude conditions where the atmospheric oxygen content, ambient pressure and temperature are greater and shear layer afterburning occurs, the chemistry effect may be significant.

4. The internozzle spacing distance has a significant impact on the barrel shock reflection location, plume/plume impingement shock location and shear layer.

Instances where these influences may impact flow field predictions occur when nozzle gimballing activities are considered.

5. A comparison of the two-dimensional and three-dimensional solutions indicates that the three-dimensional effects are important in the near-field plume and diminish as the axial distance extends farther downstream from the nozzle exit plane location. The single-equivalent-nozzle approach should not be used to describe plume near-field flow characteristics where three-dimensional plume impingement effects are dominant and in the instances where 3-D spatial features are required as part of the flow field description. In all cases, the single equivalent nozzle assumption should be carefully scrutinized. In some applications, the single equivalent nozzle assumption could be entirely inappropriate.

6. The missile body, base and gas generator flow has a significant impact on the barrel-shock-reflection location, plume/plume impingement shock location, development of the shear layer region, and the plume radial extent.

7. These analyses indicate that two-dimensional nonequilibrium analysis tools can provide some insight concerning overall gross qualitative assessments of multiple plume flow field phenomena. However, for detailed studies of complex flow field phenomena, a more sophisticated three-dimensional calculation is required.

This study is intended to assess, understand, and quantify plume physical phenomena. This insight can be applied to develop engineering application analysis tolls and identify where simplified models can be applied without compromising the validity of the solution results or the conclusions that might be deduced from analysis of the flow field simulation.

ACKNOWLEDGEMENTS

Special gratitude is extended to Ms. Martha A. Simmons for her technical support, valuable insight and assistance in preparing this paper.

REFERENCES

1. Shannan, Robert V. and Murray, Alvin, "Development of the KIVA-II CFD Code for Rocket Propulsion Applications, "Tenth Workshop for CFD Applications in Rocket Propulsion, NASA Marshall Space Flight Center, April 28-30, 1992.

2. Ebrahimi, Houshang B., "Numerical Investigation on Multi-Plume Rocket Phenomenology," 33rd AIAA Joint Propulsion Conference, AIAA-97-2942, Seattle, WA, July 6, 1997.

3. Dash S.M., and Thorpe, R. D., "Shock Capturing Model for One and Two-Phase Supersonic Exhaust Flow", AIAA Journal , Vol. 19, July 1981, pp 842-851.

4. Dash, S.M., Wolf,D.E., Beddini, R.A. and Pergament, H.S., "Analysis of Two-Phase Flow Processes in Rocket Exhaust Plumes," J. Spacecraft Rockets, Vol. 22, No.3, May-June 1985 (pp. 367-380).

5. Ebrahimi, Housing B., "Parametric Investigation of the Effect of Various Phenomena on the Performance of a Scramjet Nozzle," AIAA-95-6048, 6th International Aerospace Planes and Hypersonics, Chattanooga, TN, April 3-7, 1995.

6. Holcomb, J. Eric, "Development of an Adaptive Grid Navier-Stokes Analysis Method for Rocket Base Flows," AIAA-88-2905, Boston, MA, July 1988.

7. Van Leer, B., "Flux-Vector Splitting for the Euler Equations," in lecture note in *Physics*, Vol. 170, Springer-Verlag, 1982.

8. Ebrahimi, Houshang B., "Validation Database for Propulsion Computational Fluid Dynamics," J. Spacecraft Rockets, Vol. 34, October 1997 (pp. 642-650).

9. Nickerson, G. R., "Two-Dimensional Kinetics (TDK) Nozzle Performance Computer Program," NAS8-36863, March 1989.

10. Titan II SLV Propulsion Subsystem, 1992, Gencorp, Aerojet Propulsion Division, Sacramento, CA.

11. Jones, W. P., Launder, B. E. (1972). "The Prediction of Laminarization with a Two-equation Model of Turbulence," *International Developments in Heat Transfer*, 15, 303-314.

12. Wrisdale, Ian E., Mikulskis, David F., and Gilmore, Martin R., "Navier-Stokes Calculations of a Twin Nozzle Rocket Plume," AIAA-96-1881, Thermophysics Conference, New Orleans, LA, June 17-20, 1996.

Table 1. Parametric Flowfield Conditions

CASE	VISCOSITY	INLET PROFILE	CHEMISTRY	NOZZLE SPACING	GG
1	Laminar	1-D	Constant γ	Wide	No
2	Turbulent	1-D	Constant γ	Wide	No
3	Turbulent	1-D	Constant γ	Narrow	No
4	Turbulent	1-D	Finite Rate	Narrow	No
5	Turbulent	1-D	Frozen	Narrow	No
6	Turbulent	2-D	Finite Rate	Narrow	No
7	Turbulent	2-D	Finite Rate	Narrow	Yes
8	Turbulent	2-D	Finite Rate	2D-axisymmetric	No

Table 2. Inflow Conditions

Ambient Conditions at 47.6 km

- Tinf = 269 K
- Cp/Cv = 1.4
- P = 108 Pa
- Species Concentrations (Mass Fraction)
  N_2 = 0.77

V = 1877.6 m/sec
$\rho = 1.388 \times 10^{-3}$ kg/m^3
Mach = 5.7

O_2 = 0.23

Jet Conditions (One Dimensional)

- T = 1920 K
- P = 92800 Pa
- Mach = 3.0

V = 2776.6 m/sec
$\rho = 1.68 \times 10^{-1}$ kg/m^3

- Species Concentrations (Mass Fraction)

CO=0.039	CO_2=0.1811	H_2O=0.3496	
N_2=0.414	NO=0.0109	OH=2.139e-3	
H_2=3.13e-3	H=1.24e-4	O_2=0.0	O=0.0

Gas Generator Conditions

- M = 1.01
- T = 899 K
- P = 85488.9 Pa-
- CO = 0.04
- CO_2 = 0.004
- CH_4 = 0.135
- H_2 = 0.035
- H_2O = 0.034
- NH_3 = 0.253
- C = 0.038

T, P, and ρ are static conditions

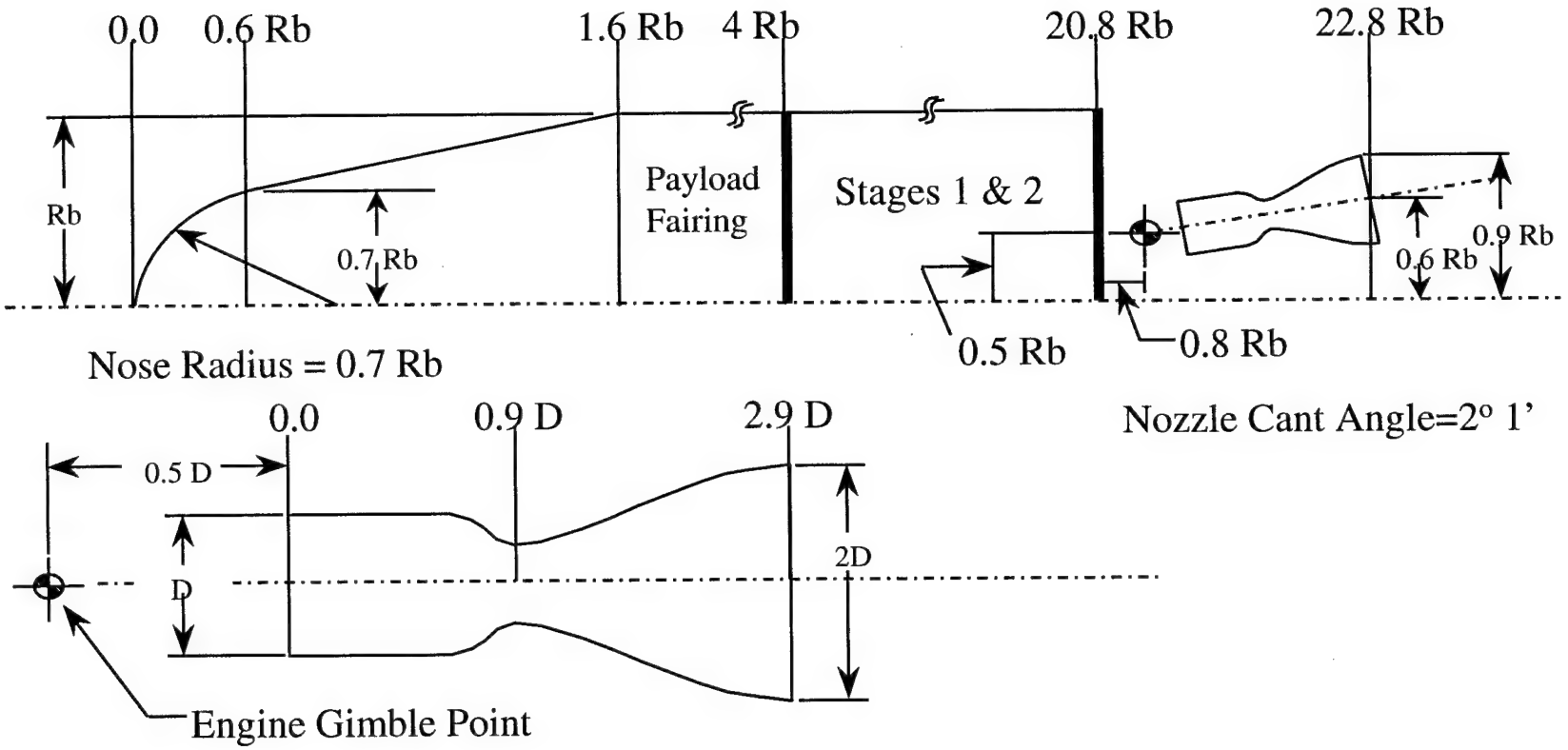

Fig. 1. Vehicle Dimensions

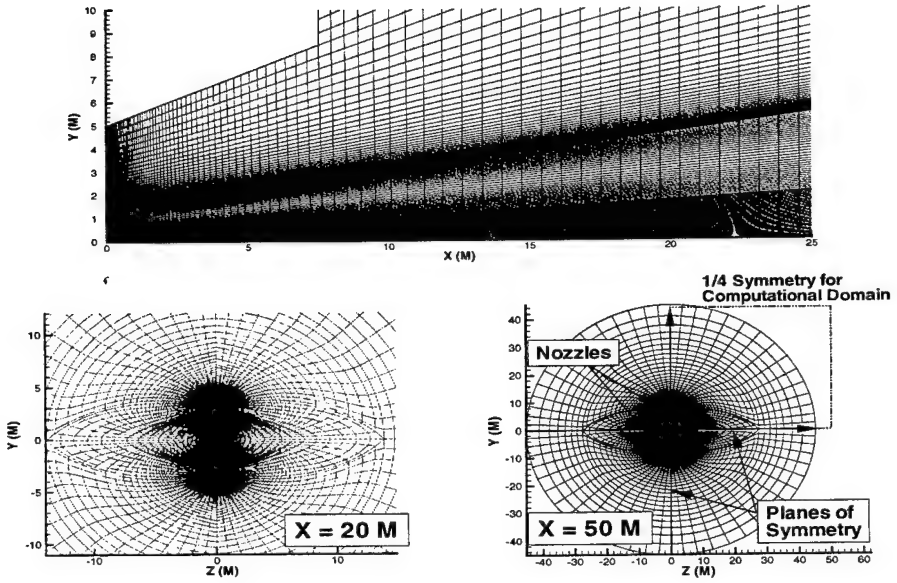

a. Schematic of the 3-D grid and the planes of symmetry.

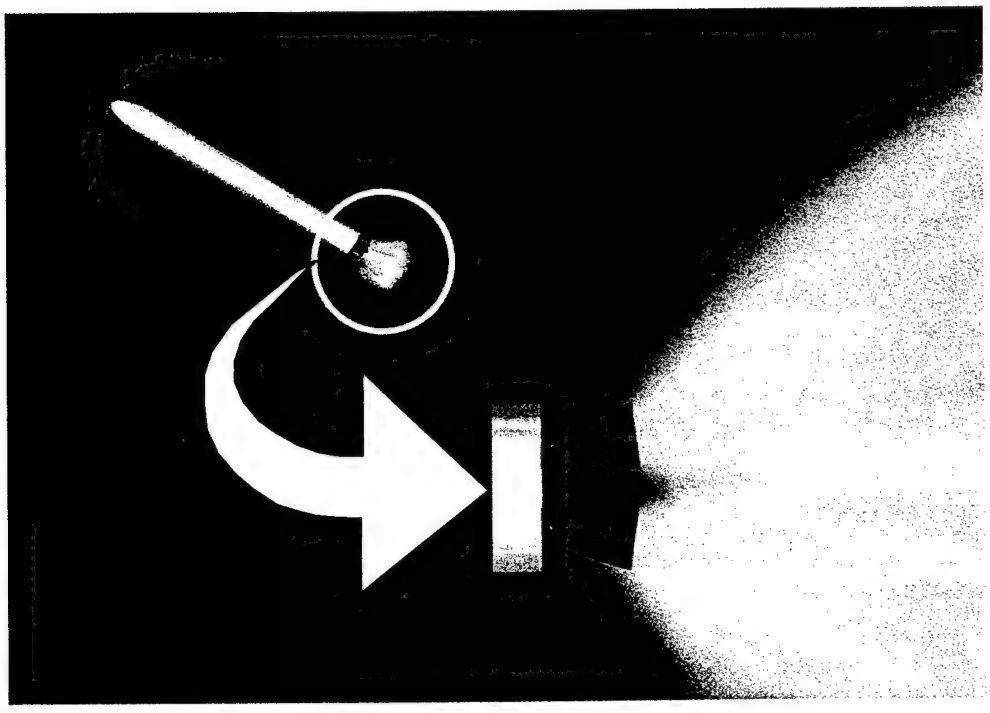

b. Notional view of the 3-D Plume

Fig 2. Geometry representation of the computational domain.

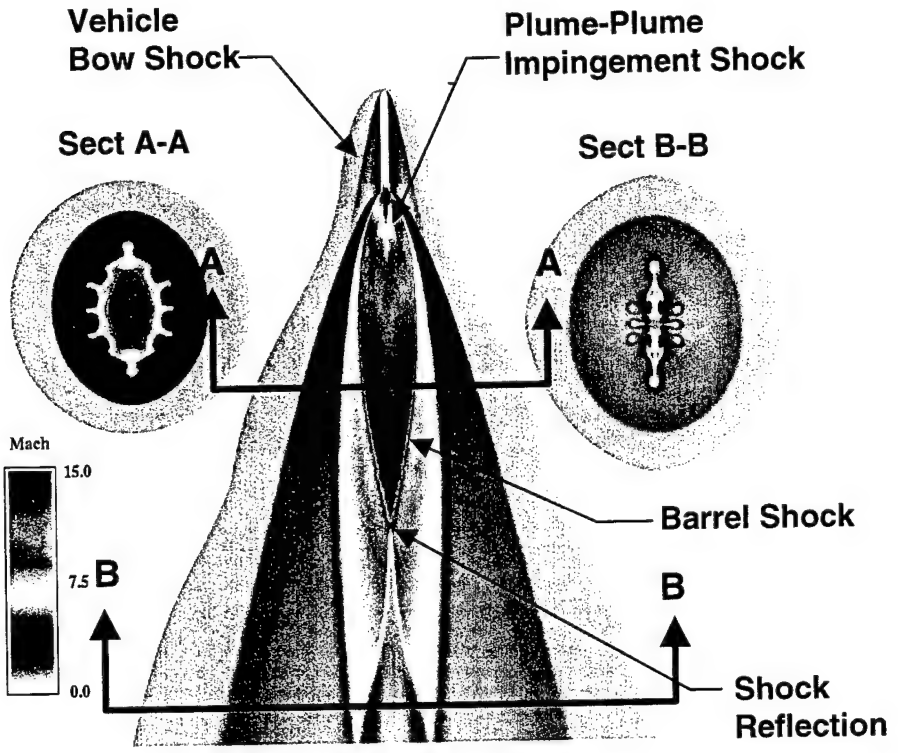

Fig. 3. Mach contours (3-D calculation).

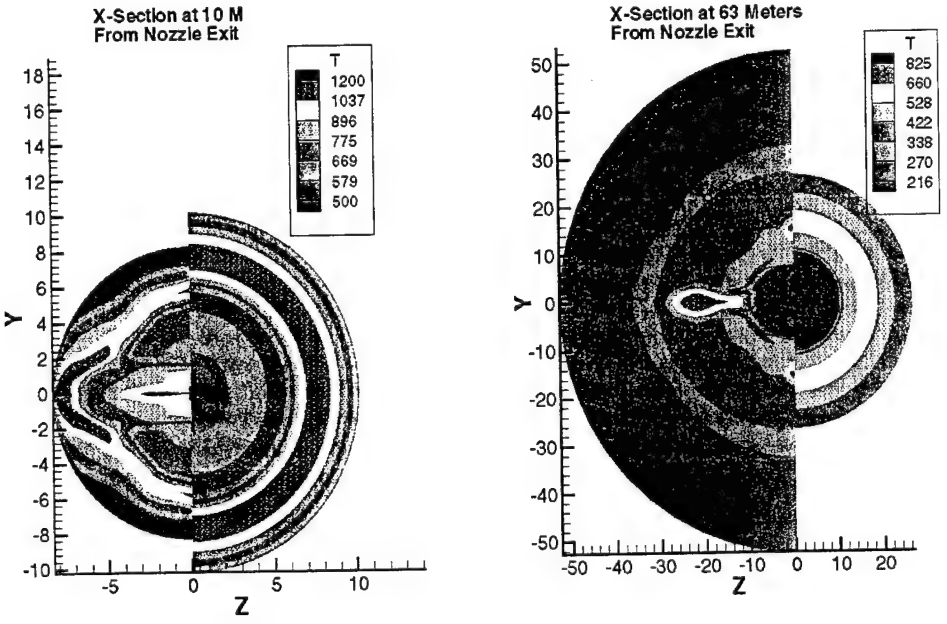

Fig. 4. Static temperature cross section comparisons, 3-D plume vs single equivalent nozzle.

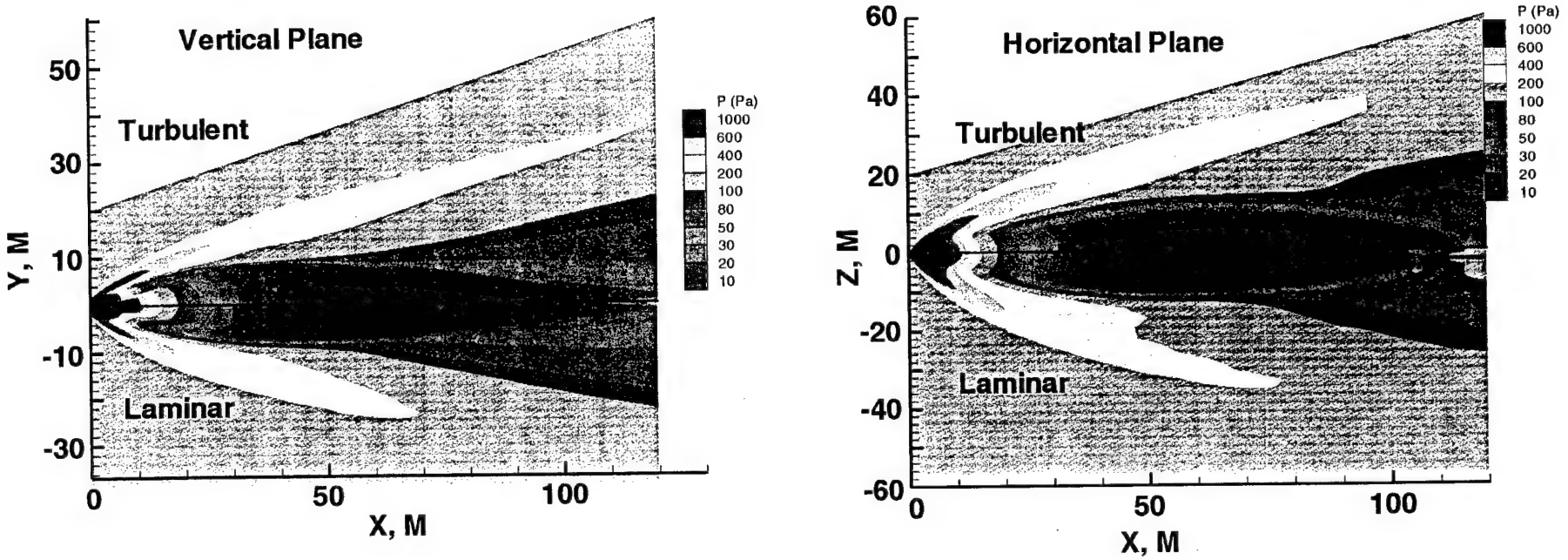

Fig. 5. Laminar and turbulent pressure comparisons.

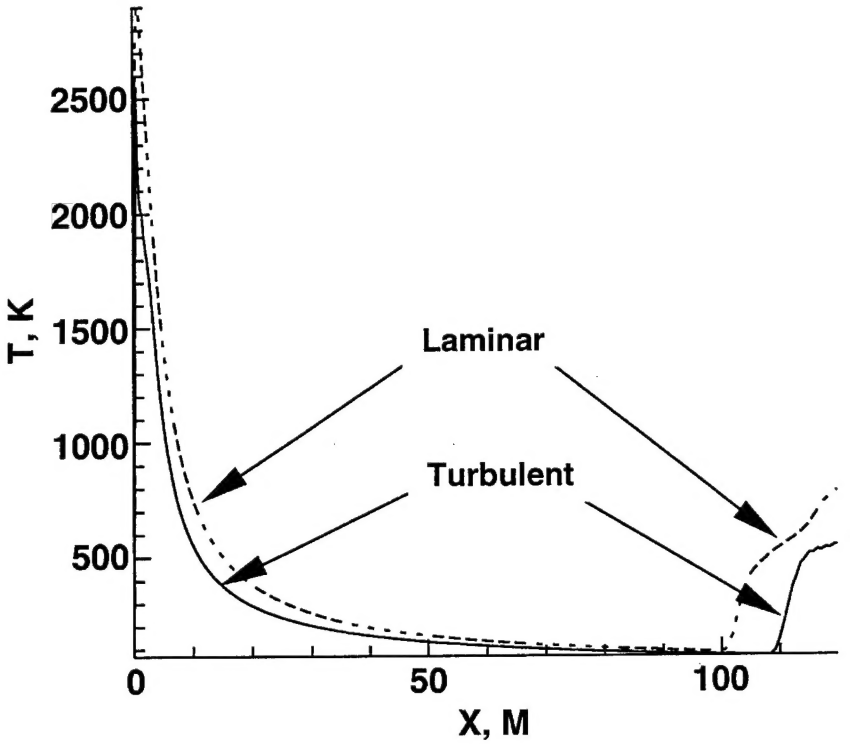

Fig. 6. Static temperature comparison along centerline.

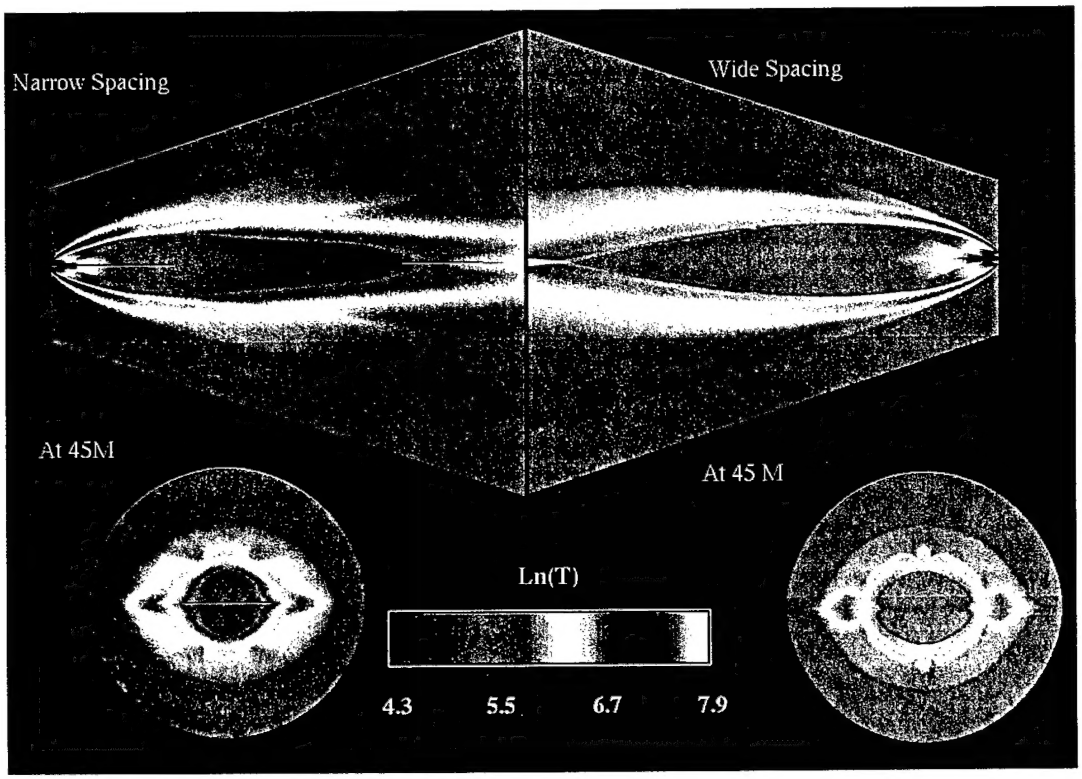

Fig. 7. Perfect gas comparisons of temperature contours illustrating nozzle spacing effects.

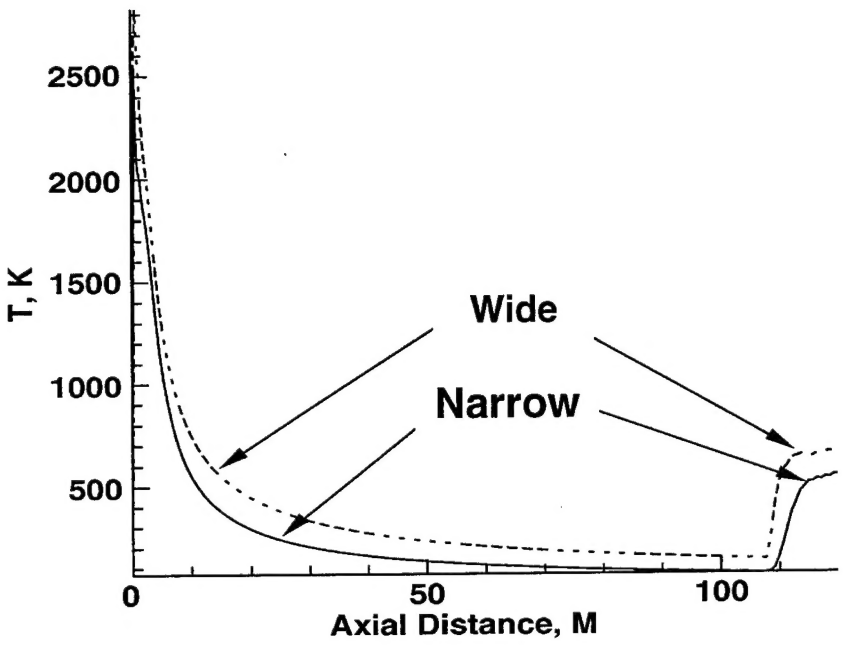

Fig. 8. X-Y plane temperatures along vehicle centerline comparing nozzle spacing effects.

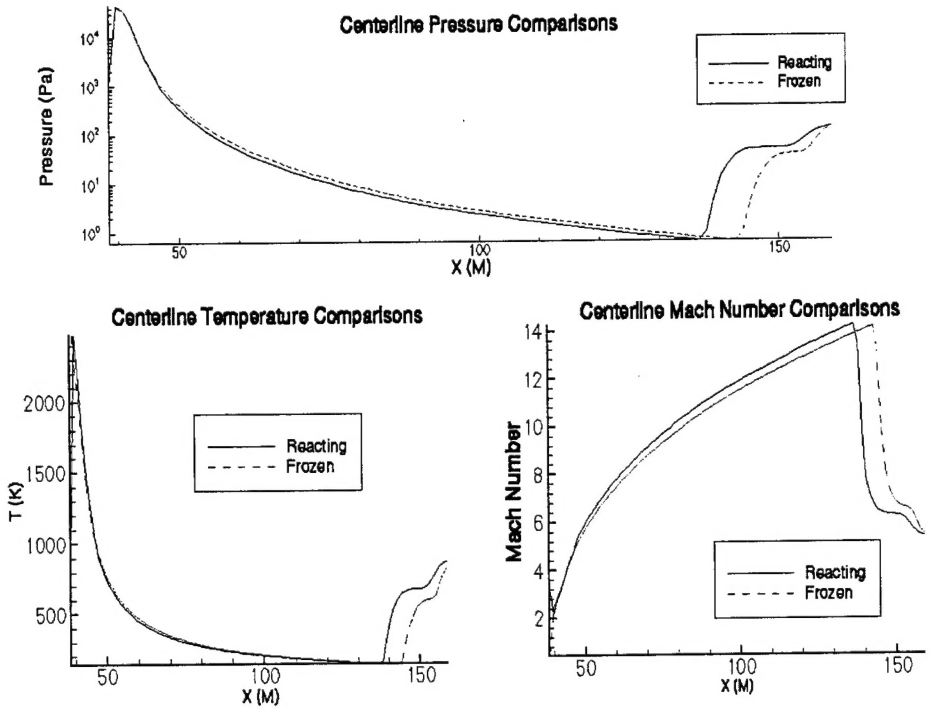

Fig. 9. Pressure, temperature, and Mach number comparison of reacting vs. frozen.

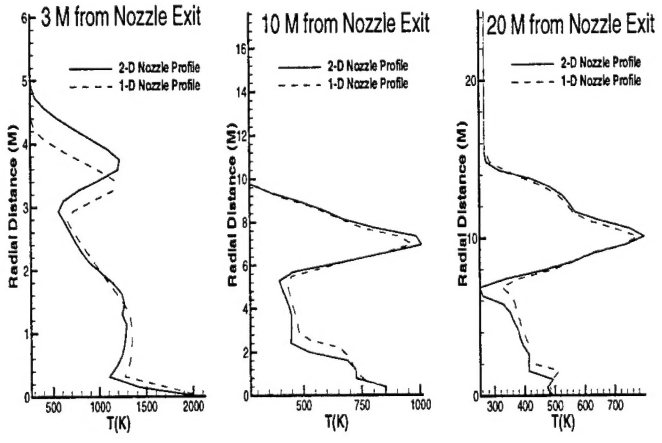

Fig. 10. Y-Z temperature profile at X=3, 10, and 20m.

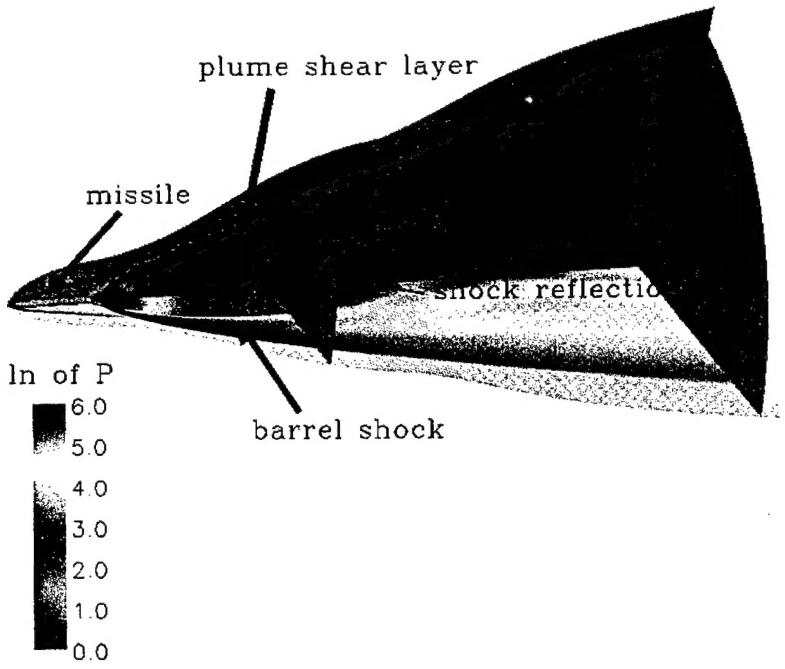

a. Pressure contours

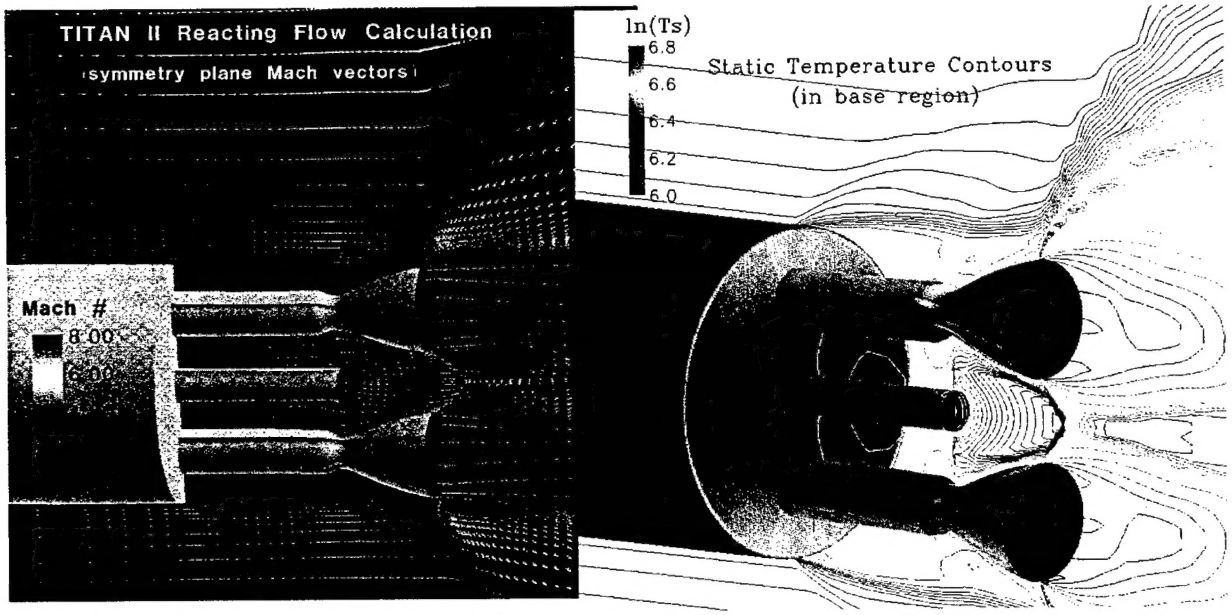

b. Mach vectors

c. Isotherms

Fig. 11. Nose-to-tail 3-D calculations